

# Evidence for a dynamically refracted primary bow in weakly bound ${}^9\text{Be}$ rainbow scattering from ${}^{16}\text{O}$

S. Ohkubo<sup>1</sup> and Y. Hirabayashi<sup>2</sup>

<sup>1</sup>*Research Center for Nuclear Physics, Osaka University, Ibaraki, Osaka 567-0047, Japan and*

<sup>2</sup>*Information Initiative Center, Hokkaido University, Sapporo 060-0811, Japan*

(Dated: November 8, 2021)

We present for the first time evidence for the existence of a dynamically refracted primary bow for  ${}^9\text{Be}+{}^{16}\text{O}$  scattering. This is demonstrated through the use of coupled channel calculations with an extended double folding potential derived from the density-dependent effective two-body force and precise microscopic cluster wave functions for  ${}^9\text{Be}$ . The calculations reproduce the experimental Airy structure in  ${}^9\text{Be}+{}^{16}\text{O}$  scattering well. It is found that coupling of a weakly bound  ${}^9\text{Be}$  nucleus to excited states plays the role of a booster lens, dynamically enhancing the refraction over the *static* refraction due to the Luneburg lens mean field potential between the ground states of  ${}^9\text{Be}$  and  ${}^{16}\text{O}$ .

PACS numbers: 25.70.Bc, 24.10.Eq, 24.10.Ht

## I. INTRODUCTION

A nuclear rainbow has been understood to be caused by refraction within the static Luneburg lens mean field potential during elastic scattering [1–3]. The existence of the nuclear rainbows has been confirmed experimentally under relatively weak absorption for many systems such as  $\alpha+{}^{40}\text{Ca}$ ,  $\alpha+{}^{16}\text{O}$ ,  ${}^{16}\text{O}+{}^{16}\text{O}$ ,  ${}^{16}\text{O}+{}^{12}\text{C}$ , and  ${}^{12}\text{C}+{}^{12}\text{C}$  [4, 5]. Very recent studies have shown the existence of a secondary bow in nuclear rainbow scattering involving  ${}^{12}\text{C}$ , which is not caused by a *static* Luneburg lens mean field potential but is generated by a *dynamical* coupling to the excited states [6, 7]. The specific structure of a strongly deformed  $\alpha$  cluster nucleus  ${}^{12}\text{C}$  is related to the dynamical generation of a secondary bow. It is therefore interesting and intriguing to investigate whether a dynamically refracted rainbow can exist in other systems for which coupling to the excited states is important.

The  ${}^9\text{Be}$  nucleus is strongly deformed with a quadrupole deformation parameter  $\beta_2=1.4$  [8], which is larger than that of  ${}^{12}\text{C}$ ,  $\beta_2=-0.40$  [9] and is weakly bound with the threshold energy 1.57 MeV, 1.67 MeV, and 2.47 MeV for the  $\alpha+\alpha+n$ ,  ${}^8\text{Be}+n$ , and  $\alpha+{}^5\text{He}$  decays, respectively. There have been extensive studies of the effect of breakup channels of weakly bound nuclei on the polarization potential [10–15]. No attention has been paid to nuclear rainbows.

The systematic study of a weakly bound  ${}^6\text{Li}$  scattering from  ${}^{12}\text{C}$  and  ${}^{16}\text{O}$  over a wide range of energies using a phenomenological potential has shown [16, 17] the existence of a nuclear rainbow and Airy structure in the angular distributions. This shows that in contrast to a naive strong absorption picture absorption of scattering involving weakly bound nuclei is not complete. As for  ${}^9\text{Be}$ , the experiment of  ${}^9\text{Be}+{}^{16}\text{O}$  scattering in the rainbow energy region was performed at  $E({}^9\text{Be})=157.7$  MeV [18, 19]. Satchler *et al.* [18] interpreted that the observed rainbow-like behavior of the angular distribution is a nuclear rainbow “ghost”. Khoa [20] reproduced the angular distribution of the nuclear rainbow “ghost” using double folding model calculations with the M3Y force well by

taking into account the finite-range exchange effect. Recently Glukhov *et al.* [21] measured  ${}^{16}\text{O}+{}^9\text{Be}$  scattering at  $E({}^{16}\text{O})=132$  MeV and reported the existence of an Airy minimum in the phenomenological optical model analysis.

It is important to definitively confirm the existence of a nuclear rainbow theoretically and also to investigate how a rainbow is generated in weakly bound  ${}^9\text{Be}$  scattering. The relevance of the breakup to the emergence of a nuclear rainbow is especially important. Also it is intriguing to investigate whether a double folding model derived from the density-dependent force, which has been successful in many systems involving non-weakly bound nuclei such as  $\alpha$  particle,  ${}^{16}\text{O}$ ,  ${}^{12}\text{C}$ , and  ${}^{14}\text{C}$  [5, 22–25], can describe the nuclear rainbow phenomenon involving a weakly bound  ${}^9\text{Be}$  nucleus well.

The purpose of this paper is to present for the first time evidence for the existence of a dynamically refracted primary bow by studying the mechanism of generation of a nuclear rainbow in scattering of a weakly bound  ${}^9\text{Be}$  nucleus from  ${}^{16}\text{O}$ . Coupled channel calculations with an extended double folding model potential derived from the precise wave functions of  ${}^9\text{Be}$  and the density-dependent effective force are performed. It is shown that refraction is boosted by coupling to the excited states. This boosted dynamical refraction in addition to the static refraction in the mean field potential manifests itself in the observation of a primary bow in nature.

## II. EXTENDED DOUBLE FOLDING MODEL

We study  ${}^9\text{Be}+{}^{16}\text{O}$  scattering using the coupled channel (CC) method with an extended double folding (EDF) model that describes all the diagonal and off-diagonal coupling potentials derived from a density-dependent nucleon-nucleon force and the precise microscopic wave functions for  ${}^9\text{Be}$  and  ${}^{16}\text{O}$ . The diagonal and coupling potentials for the  ${}^9\text{Be}+{}^{16}\text{O}$  system are calculated using

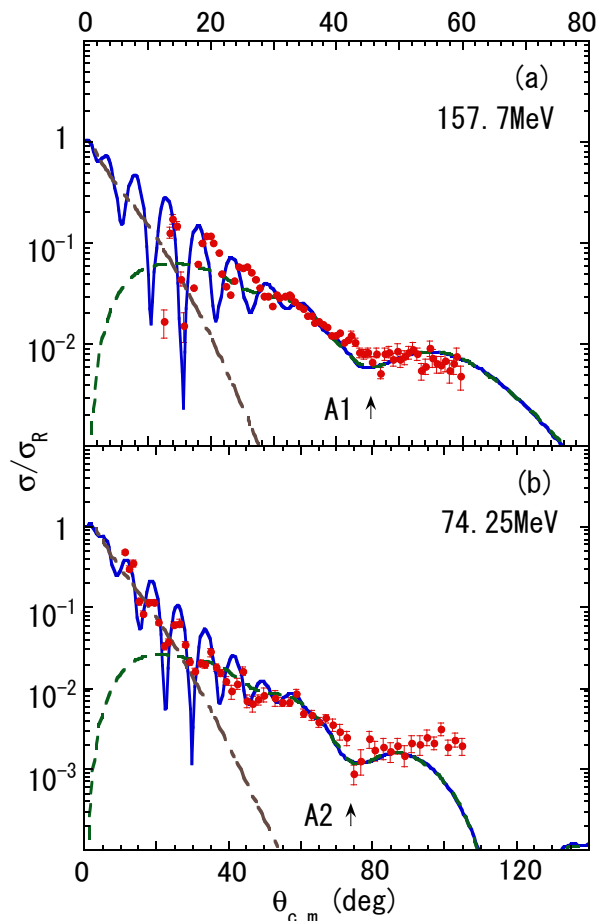


FIG. 1: (Color online) The angular distributions of  ${}^9\text{Be}+{}^{16}\text{O}$  scattering at (a)  $E({}^9\text{Be})=157.7$  MeV and (b)  $74.25$  MeV ( $E({}^{16}\text{O})=132$  MeV) calculated in a single channel (solid lines) are compared with the experimental data (points) [18, 19, 21]. The calculated cross sections are decomposed into the farside component (dashed lines) and the nearside component (dash-dotted lines).

the EDF model

$$V_{ij}(\mathbf{R}) = \int \rho_{ij}^{({}^9\text{Be})}(\mathbf{r}_1) \rho^{({}^{16}\text{O})}(\mathbf{r}_2) \times v_{NN}(E, \rho, \mathbf{r}_1 + \mathbf{R} - \mathbf{r}_2) d\mathbf{r}_1 d\mathbf{r}_2, \quad (1)$$

where  $\rho_{ij}^{({}^9\text{Be})}(\mathbf{r})$  represents the diagonal ( $i = j$ ) or transition ( $i \neq j$ ) nucleon density of  ${}^9\text{Be}$  which is calculated using the microscopic molecular model in the generator coordinate method [26]. This model reproduces the energy spectra, electromagnetic properties, charge form factors, neutron and  $\alpha$  decay widths of  ${}^9\text{Be}$  well [26]. In the coupled channel calculations we include the ground band states of  ${}^9\text{Be}$ ,  $3/2^-$  (0.0 MeV),  $5/2^-$  (2.43 MeV) and  $7/2^-$  (6.38 MeV) [27]. Other states (for example,  $1/2^+$  (1.68 MeV),  $1/2^-$  (2.78 MeV) and  $5/2^+$  (3.05 MeV)) are found not to contribute significantly in the present coupled channel calculations.  $\rho^{({}^{16}\text{O})}(\mathbf{r})$  is the nucleon density of  ${}^{16}\text{O}$  taken from Ref.[28]. For the effective in-

TABLE I: The normalization factor  $N_R$ , volume integral per nucleon pair  $J_V$  of the the ground state diagonal potential (in units of  $\text{MeVfm}^3$ ), and the imaginary potential parameters used in the single channel double folding calculations and coupled channel calculations with EDF in Fig. 1 and Fig. 2.

| $E({}^9\text{Be})$ | $E({}^{16}\text{O})$ | (single channel cal) |       |      |      | (coupled channel cal) |       |     |      |
|--------------------|----------------------|----------------------|-------|------|------|-----------------------|-------|-----|------|
|                    |                      | $N_R$                | $J_V$ | $W$  | $a$  | $N_R$                 | $J_V$ | $W$ | $a$  |
| (MeV)              | (MeV)                |                      | (MeV) | (fm) |      | (MeV)                 | (fm)  |     | (fm) |
| 74.25              | 132                  | 1.1                  | 393   | 21   | 0.9  | 1.03                  | 368   | 17  | 1.0  |
| 157.7              | 280.4                | 1.1                  | 356   | 24   | 0.95 | 1.00                  | 324   | 20  | 1.0  |

teraction  $v_{NN}$  we use the Density Dependent Michigan 3 range Yukawa-Finite Range (DDM3Y-FR) interaction [29], which takes into account the finite-range nucleon exchange effect [30]. We introduce the normalization factor  $N_R$  [31, 32] for the real double folding potential. An imaginary potential with a Woods-Saxon volume-type (nondeformed) form factor is introduced phenomenologically to take into account the effect of absorption due to other channels. A complex coupling, which is often used but has no rigorous theoretical justification especially for a composite projectile [33], is not introduced because without it the present EDF model successfully reproduced many rainbow scattering data systematically over a wide range of incident energies [6, 7, 22, 23, 34–39].

### III. ANALYSIS OF ${}^9\text{Be} + {}^{12}\text{C}$ SCATTERING

We analyze the angular distributions of  ${}^9\text{Be}+{}^{16}\text{O}$  scattering at  $E({}^9\text{Be})=157.7$  MeV ( $E_{c.m.}=100.9$  MeV) [18, 19] and  $E({}^{16}\text{O})=132$  MeV ( $E_{c.m.}=47.5$  MeV,  $E({}^9\text{Be})=74.25$  MeV) [21] in the rainbow energy region. Hereafter, the incident energies are given in the frame of  $E({}^9\text{Be})$ . In Fig. 1 the angular distributions calculated in a single channel are displayed in comparison with the experimental data. In the calculations the reorientation of the ground state is not included. The value of  $N_R$  for the real potential was adjusted to fit the data. For the imaginary potential a radius parameter was fixed at  $R=5.5$  fm while a strength parameter of around  $W=20$  MeV and a diffuseness parameter of around  $a = 1.0$  fm were found to fit the data. The values of  $N_R$  together with the volume integral per nucleon pair of the real potential,  $J_V$ , and potential parameters are given in Table I. The characteristic features of a nuclear rainbow scattering in the experimental angular distributions are reproduced well by the calculations by only slightly changing the value of  $N_R$  from unity to  $N_R=1.1$ . The calculated cross sections are decomposed into the farside and nearside contributions. The angular distributions at the forward angles are Fraunhofer diffractive scattering, which are sensitive only to the surface region of the potential [15], and in the present calculations they are caused by the interference

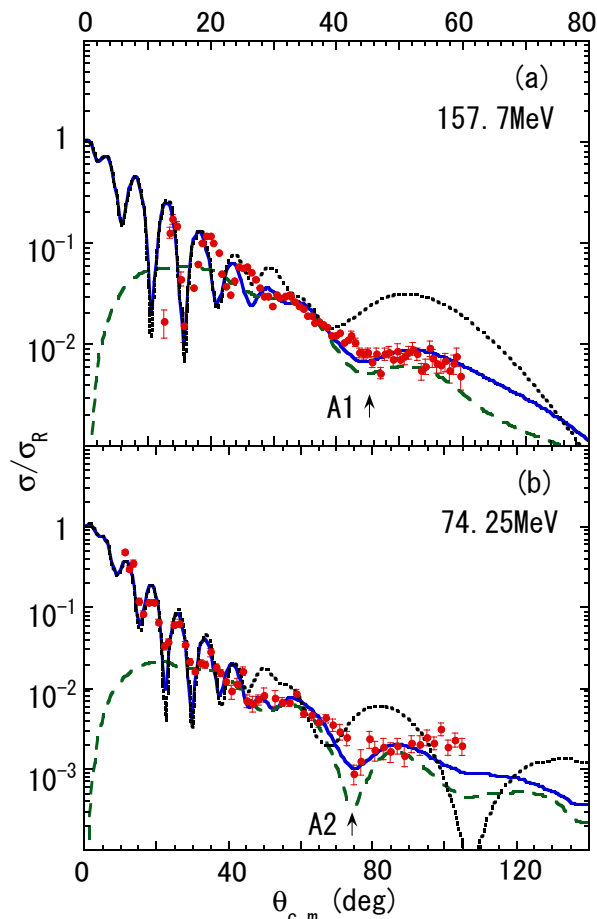


FIG. 2: (Color online) The angular distributions of  ${}^9\text{Be}+{}^{16}\text{O}$  scattering at (a)  $E({}^9\text{Be})=157.7$  MeV and (b) 74.25 MeV ( $E({}^{16}\text{O})=132$  MeV) calculated using the coupled channel method with coupling to both the  $5/2^-$  and  $7/2^-$  states including reorientations (solid lines) are compared with the experimental data (points) [18, 19, 21]. The farside component of the calculated cross sections is indicated by the dashed lines. The single channel calculations where the coupling is switched off are displayed for comparison with dotted lines.

between the nearside and farside contributions as seen in Fig. 1. On the other hand, the angular distributions in the intermediate angular region are dominated by only farside refractive scattering, which penetrates deep into the internal region of the potential. Thus the minima in the experimental angular distributions at  $\theta = 45^\circ$  in Fig. 1(a) and  $78^\circ$  in Fig. 1 (b) are found to be Airy minima of the nuclear primary rainbow. At 157.7 MeV in Fig. 1(a) the calculation reproduces the Airy minimum in agreement with the experimental minimum. The Airy minimum at  $\theta = 45^\circ$  and the Airy maximum at around  $\theta = 55^\circ$  are assigned to be of first order, A1 because beyond that there is a fall-off in the angular distribution, which is the appearance of the darkside of a nuclear rainbow. Although the fall-off has not been measured in experiment, it is clear that the minimum and maximum are not the “ghost” of the nuclear rainbow but the real

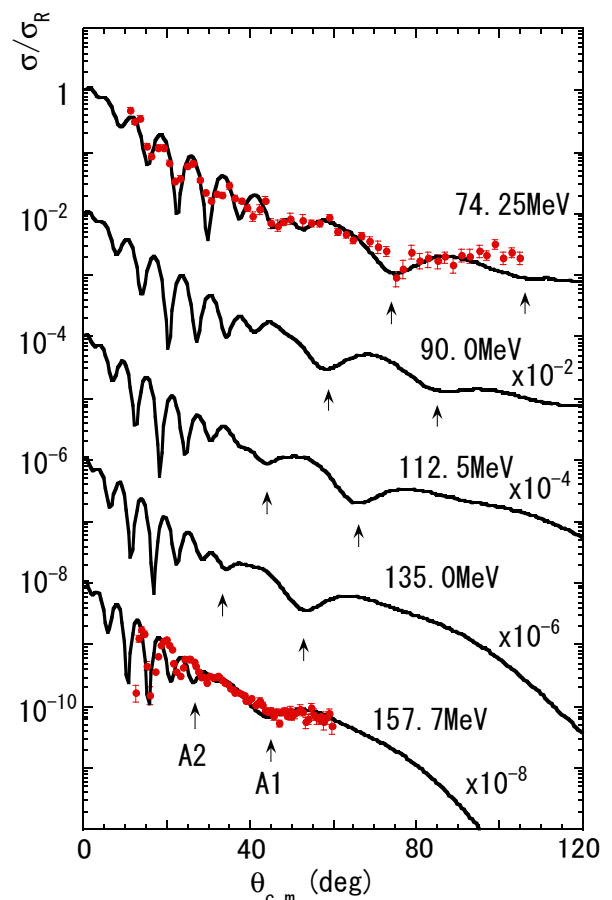


FIG. 3: (Color online) The energy evolution of the Airy minimum A1 and A2 of the Airy structure in the angular distributions between  $E({}^9\text{Be})=157.7$  MeV and 74.25 MeV ( $E({}^{16}\text{O})=132$  MeV), calculated using the CC method, are displayed with solid lines. The experimental data [18, 19, 21] are indicated by the points.

rainbow due to refractive scattering. That this is really the nuclear rainbow can be further confirmed in the lower energy experimental data at 74.25 MeV in Fig. 1(b) by identifying the existence of the higher order Airy minimum of the nuclear primary rainbow. The calculation reproduces the characteristic features of the experimental angular distribution with a minimum at  $78^\circ$ , which is a second order Airy minimum A2 well. This order will be shown without ambiguity by investigating the energy evolution of the angular position of the Airy minimum, as displayed in Fig. 3. Some enhancement of the experimental cross sections beyond  $\theta = 90^\circ$  at 74.25 MeV compared with the calculation may be due to effects other than refractive scattering such as exchange effects.

In order to reveal the role of the excited states on the emergence of the primary nuclear rainbow, the angular distributions of elastic  ${}^9\text{Be}+{}^{16}\text{O}$  scattering calculated using the coupled channel method including reorientations are displayed in Fig. 2. For the imaginary potential, the strength parameter  $W$  is slightly readjusted to decrease

because of channel coupling while the radius parameter was kept  $R = 5.5$  fm. The values of  $N_R$  needed are almost unity and slightly smaller than those in the single channel calculations in Fig. 1. The potential parameters used and the values of the volume integral per nucleon pair of the double folding potential,  $J_V$ , are given in Table I. The CC calculations reproduce the Airy structure of the experimental angular distributions well. In Fig. 2(a) the minimum  $A1$  at  $\theta = 45^\circ$  is seen to be caused by farside refractive scattering also in the coupled channel calculation. In the calculation without coupling (dotted lines), although the Airy minimum  $A1$  is seen, it is located at a considerably smaller angle  $\theta = 38^\circ$  in disagreement with the experimental  $\theta = 45^\circ$ . This means the attraction is insufficient without coupling to the excited states. By introducing coupling to the excited states, the Airy minimum  $A1$  moves backward in agreement with the experimental data as seen in Fig. 2(a). In Fig. 2(b) the same situation is seen at the lower energy of  $E(^9\text{Be})=74.25$  MeV. The experimental Airy minimum  $A2$  at  $\theta = 78^\circ$  is correctly reproduced by the CC calculation. The dominance of the farside contribution in the CC calculation in the intermediate angular region shows that this minimum is really an Airy minimum due to refractive scattering. In the calculation without channel coupling (dotted lines), although the Airy minimum  $A2$  is seen, it is located considerably farther forward, at an angle  $\theta = 65^\circ$ . This means that attraction is lacking considerably if the coupling to the excited states are absent. Thus it is found that coupling to the excited  $5/2^-$  and  $7/2^-$  states plays the role of inducing additional attraction. Namely, the coupling plays the role of a booster second lens causing additional refraction over that due to the static Luneburg lens mean field potential caused by the ground state. Thus the emergence of the primary nuclear rainbow for this system is found to be realized in nature by the dynamically boosted refraction due to the coupling to the excited states.

In Fig. 3 the energy evolution of the Airy structure for  $^9\text{Be}+^{16}\text{O}$  scattering is shown, by displaying the angular distributions for a range of energies between  $E(^9\text{Be})=157.7$  and  $74.25$  MeV. The angular distributions are calculated in the three coupled channel calculations using the interpolated potential parameters. The angular position of the Airy minimum moves backward as the energy decreases. The  $A1$  located at  $\theta = 45^\circ$  at  $157.7$  MeV moves backward to  $105^\circ$  at  $74.25$  MeV, whose existence could be confirmed by measurement at larger angles. On the other hand, the  $A2$  that is located at forward angles at  $157.7$  MeV, and which is difficult to see in the experimental data due to being masked by the Fraunhofer diffraction, develops moving backward as the incident energy decreases. At  $74.25$  MeV this Airy minimum is clearly identified as that of order two,  $A2$ , at  $\theta = 78^\circ$  in the experimental angular distribution. Thus the existence of a nuclear rainbow together with the higher order Airy structure is confirmed for scattering involving a weakly bound  $^9\text{Be}$  nucleus.

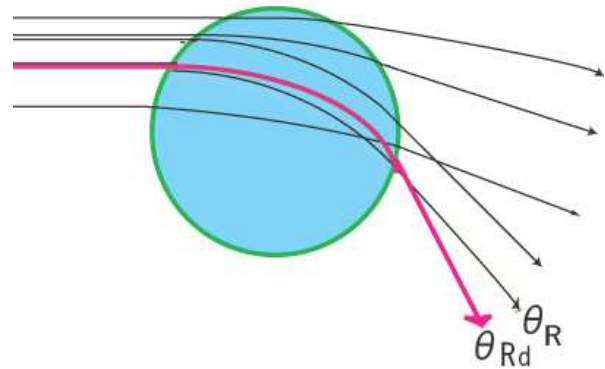


FIG. 4: (Color online) Illustrative refractive trajectories (solid lines) in nuclear rainbow scattering. The refracted angle  $\theta_R$  is a rainbow angle for the primary nuclear rainbow caused by the mean field optical potential (Luneburg lens [3]) of the nucleus (indicated by a circle) without coupling to the excited states. The angular region  $\theta < \theta_R$  is the bright side of the primary nuclear rainbow and  $\theta > \theta_R$  is the darkside. By coupling to the excited states of  $^9\text{Be}$  the refraction is dynamically enhanced and the rainbow angle is increased to  $\theta_{Rd}$ .

#### IV. PRIMARY BOW AND BOOSTER LENS

In Fig. 4 an illustrative figure of the enhanced refraction, boosted dynamically by coupling to excited states of  $^9\text{Be}$ , is displayed. The incident projectile is refracted by the static potential due to the ground state of the target nucleus  $^{16}\text{O}$ . The largest refractive angle (rainbow angle, deflection angle) in the static potential is indicated by  $\theta_R$ . Because the projectile is easily excited, the strong coupling to the excited states of the ground band above the threshold energy for breakup causes additional refraction. Thus the largest refractive angle is increased to  $\theta_{Rd}$ . The excited states play the role of a dynamical booster lens, enhancing the refraction over the static refraction caused by the Luneburg lens mean field ground state potential. The observed rainbow may be called a dynamically refracted rainbow or a dynamically boosted rainbow because it is not realized in nature without this boosting. From Table I, we can determine quantitatively the induced attraction by considering changes of the value of  $J_V$ :  $\Delta J_V=25$  MeVfm<sup>3</sup> at  $157.7$  MeV and  $\Delta J_V=32$  MeVfm<sup>3</sup> at  $74.25$  MeV. About 10% of the refraction is due to dynamical effects.

In order to confirm the dynamical refraction we have also calculated by using other effective forces. Hitherto we have shown the results calculated by using the DDM3Y force with a density-dependence of Kobos type [29], which has been successful for many calculations of nuclear rainbow scattering [6, 7, 22, 23, 34–39]. The  $\chi^2$  values at  $74.25$  MeV ( $157.7$  MeV) for the single channel (Fig. 1) and coupled channel (Fig. 2) calculations are  $4.2$  ( $8.4$ ) and  $2.4$  ( $6.6$ ), respectively, at  $\theta > 45^\circ$  ( $\theta > 30^\circ$ ). We show in Fig. 5 the calculated results using the zero-range

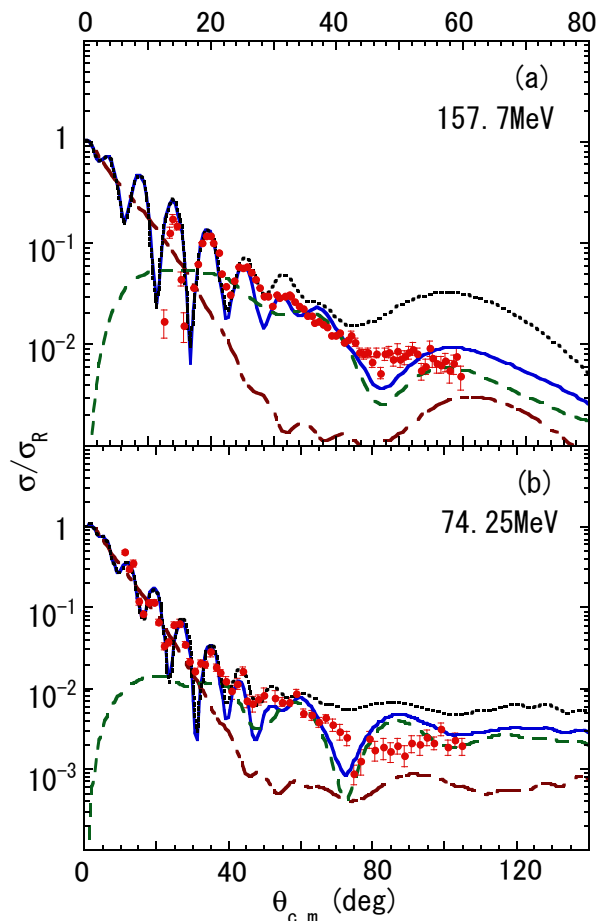


FIG. 5: (Color online) Same as Fig. 2 but for the calculations with the M3Y force. The angular distributions of  ${}^9\text{Be}+{}^{16}\text{O}$  scattering at (a)  $E({}^9\text{Be})=157.7$  MeV and (b) 74.25 MeV ( $E({}^{16}\text{O})=132$  MeV) calculated using the coupled channel method with coupling to both the  $5/2^-$  and  $7/2^-$  states including reorientations (solid lines) are compared with the experimental data (points) [18, 19, 21]. The farside and nearside component of cross sections calculated using the CC method are indicated with dashed lines and dashed-dotted lines, respectively. The single channel calculations where the coupling is switched off are displayed for comparison with dotted lines.

M3Y force, which reproduce well the phases of the angular distribution of the Fraunhofer diffraction at forward angles in agreement with the experiment at 157.7 MeV as well as at 74.25 MeV. The improvement of the phases is due a slightly shallower potential in the surface region. The used potential parameters are  $N_R=0.70$ ,  $W=18$  MeV and  $a=0.85$  fm for 157.7 MeV and  $N_R=0.92$ ,  $W=15$  MeV and  $a=1.0$  fm for 74.25 MeV with a fixed  $R=5.5$  fm. That the primary bow is boosted dynamically by the coupling to the excited states of  ${}^9\text{Be}$  does not change in the calculations using M3Y force. The calculations using the DDM3Y force with zero-range also supports this conclusion.

## V. SUMMARY

To summarize, we have presented evidence for the existence of a primary bow refracted dynamically by coupling to the excited states of a weakly bound  ${}^9\text{Be}$  nucleus. The excited states play the role of a booster lens. This is demonstrated by analyzing  ${}^9\text{Be}+{}^{16}\text{O}$  rainbow scattering using the coupled channel method with an extended double folding (EDF) potential derived from the density-dependent effective two-body force with precise microscopic cluster wave functions for  ${}^9\text{Be}$ . The calculations reproduce the Airy structure in the experimental angular distributions of  ${}^9\text{Be}+{}^{16}\text{O}$  rainbow scattering well and clearly identify the existence of the Airy minimum A1 and the higher order Airy minimum A2. About 10% of the refraction is due to dynamical effects.

## VI. ACKNOWLEDGEMENTS

The authors thank the Yukawa Institute for Theoretical Physics, Kyoto University for the hospitality extended during a stay in February 2016 where this work was completed.

- 
- [1] K. W. Ford and J. A. Wheeler, *Ann Phys.* **7**, 259 (1959).
  - [2] D. M. Brink, *Semi-classical Methods for Nucleus-Nucleus Scattering* (Cambridge University Press, Cambridge, 1985).
  - [3] F. Michel, G. Reidemeister, and S. Ohkubo, *Phys. Rev. Lett.* **89**, 152701 (2002).
  - [4] D. A. Goldberg and S. M. Smith, *Phys. Rev. Lett.* **29**, 500 (1972); D. A. Goldberg, S. M. Smith, and G. F. Burdzik, *Phys. Rev. C* **10**, 1362 (1974).
  - [5] D. T. Khoa, W. von Oertzen, H. G. Bohlen, and S. Ohkubo, *J. Phys. G* **34**, R111 (2007) and references therein.
  - [6] S. Ohkubo and Y. Hirabayashi, *Phys. Rev. C* **89**, 051601(R) (2014).
  - [7] S. Ohkubo, Y. Hirabayashi, and A. A. Ogloblin, *Phys. Rev. C* **92**, 051601 (2015) and references therein.
  - [8] S. Tanaka, K. Fukunaga, S. Kakigi, T. Ohsawa, N. Fujiwara, and T. Yanabu, *J. Phys. Soc. Jpn.* **45**, 733 (1978).
  - [9] M. Yasue *et al.*, *Nucl. Phys.* **A394**, 29 (1983).
  - [10] I. J. Thompson and M. A. Nagarajan, *Phys. Lett.* **B106**, 163 (1981).
  - [11] M. A. Nagarajan, I. J. Thompson, and R. C. Johnson, *Nucl. Phys.* **A385**, 525 (1982).
  - [12] J. Gomez-Camacho, M. Lozano, and M.A. Nagarajan, *Phys. Lett. B*, **161**, 39 (1985).
  - [13] Y. Sakuragi, M. Yahiro, and M. Kamimura, *Prog. Theor. Phys.* **70**, 1047 (1983); *Prog. Theor. Phys. Suppl.* **89**, 136 (1989) and references therein.

- [14] Y. Sakuragi, Phys. Rev. C **35**, 2161 (1987).
- [15] Y. Hirabayashi, S. Okabe, and Y. Sakuragi, Phys. Lett. **B221**, 227 (1989).
- [16] F. Michel and S. Ohkubo, Phys. Rev. C **72**, 054601 (2005).
- [17] F. Michel and S. Ohkubo, Eur. Phys. J. Special Topics **150**, 41 (2007).
- [18] G. R. Satchler, C. B. Fulmer, R. L. Auble, J. B. Ball, F. E. Bertrand, K. A. Erb, E. E. Gross, and D. C. Hensley, Phys. Lett. **B128**, 147 (1983).
- [19] C. B. Fulmer, G. R. Satchler, K. A. Erb, D. C. Hensley, R. L. Auble, J. R. Ball, F. E. Bertrand, and E. E. Gross, Nucl. Phys. **A427**, 545 (1984).
- [20] D. T. Khoa, Nucl. Phys. **A484**, 376 (1988).
- [21] Yu. A. Glukhov, A. A. Ogloblin, K. P. Artemov, and V. P. Rudakov, Phys. At. Nucl. **73**, 14 (2010).
- [22] Y. Hirabayashi and S. Ohkubo, Phys. Rev. C **88**, 014314 (2013).
- [23] S. Ohkubo and Y. Hirabayashi, Phys. Rev. C **92**, 024624 (2015).
- [24] U. Atzrott, P. Mohr, H. Abele, C. Hillenmayer, and G. Staudt, Phys. Rev. C **53**, 1336 (1996).
- [25] H. Abele and G. Staudt, Phys. Rev. C **47**, 742 (1993).
- [26] S. Okabe, Y. Abe, and H. Tanaka, Prog. Theor. Phys. **57**, 866 (1977); S. Okabe and Y. Abe, Prog. Theor. Phys. **59**, 315 (1978); Prog. Theor. Phys. **61**, 1049 (1979).
- [27] D. R. Tilley, J. H. Kelley, J. L. Godwin, D. J. Millener, J. E. Purcell, C. G. Sheu, and H. R. Weller, Nucl. Phys. **A745**, 155 (2004).
- [28] S. Okabe, *Tours Symposium on Nuclear Physics II*, edited by H. Utsunomiya *et al.* (World Scientific, Singapore, 1995), p. 112.
- [29] A. M. Kobos, B. A. Brown, P. E. Hodgson, G. R. Satchler, and A. Budzanowski, Nucl. Phys. **A384**, 65 (1982); A. M. Kobos, B. A. Brown, R. Lindsay, and G. R. Satchler, Nucl. Phys. **A425**, 205 (1984). G. Bertsch, J. Borysowicz, H. McManus, and W. G. Love, Nucl. Phys. **A284**, 399 (1977).
- [30] D. T. Khoa, W. von Oertzen, and H. G. Bohlen, Phys. Rev. C **49**, 1652 (1994).
- [31] D. T. Khoa, Phys. Rev. C **63**, 034007 (2001).
- [32] M. E. Brandan and G. R. Satchler, Phys. Rep. **285**, 143 (1997).
- [33] G. R. Satchler, *Direct Nuclear Reactions* (Oxford University Press, Oxford, 1983).
- [34] S. Ohkubo and Y. Hirabayashi, Phys. Rev. C **89**, 061601(R) (2014).
- [35] S. Ohkubo, Y. Hirabayashi, A. A. Ogloblin, Yu. A. Gloukhov, A. S. Dem'yanova, and W. H. Trzaska, Phys. Rev. C **90**, 064617 (2014).
- [36] R. S. Mackintosh, Y. Hirabayashi, and S. Ohkubo, Phys. Rev. C **91**, 024616 (2015).
- [37] S. Ohkubo and Y. Hirabayashi, Phys. Rev. C **70**, 041602 (R) (2004).
- [38] S. Ohkubo and Y. Hirabayashi, Phys. Rev. C **75**, 044609 (2007).
- [39] Sh. Hamada, Y. Hirabayashi, N. Burtbayev, and S. Ohkubo, Phys. Rev. C **87**, 024311 (2013).